

Fermi-LAT discovery of the GeV emission of the superluminous supernovae SN 2017egm

Shang Li,¹ Yun-Feng Liang,² Neng-Hui Liao,³ Lei Lei,^{4,5} and Yi-Zhong Fan^{4,5,*}

¹*School of Physics and Optoelectronics Engineering, Anhui University, Hefei 230601, China*

²*Laboratory for Relativistic Astrophysics, Department of Physics, Guangxi University, Nanning 530004, China*

³*Department of Physics and Astronomy, College of Physics, Guizhou University, Guiyang 550025, China*

⁴*Key Laboratory of Dark Matter and Space Astronomy of Chinese Academy of Sciences, Nanjing 210023, China*

⁵*School of Astronomy and Space Science, University of Science and Technology of China, Hefei 230026, China*

Superluminous supernovae (SLSNe) are a new class of transients with luminosities $\sim 10 - 100$ times larger than the usual core-collapse supernovae (SNe). Their origin is still unclear and one widely discussed scenario involves a millisecond magnetar central engine. The GeV-TeV emission of SLSNe has been predicted in the literature but has not been convincingly detected yet. Here we report the search for the γ -ray emission in the direction of SN 2017egm, one of the closest SLSNe detected so far, with the 15-year *Fermi*-LAT Pass 8 data. There is a transient γ -ray source appearing about 2 months after this event and lasting a few months. Both the peak time and the luminosity of the GeV emission are consistent with the magnetar model prediction, suggesting that such a GeV transient is the high-energy counterpart of SN 2017egm and the central engine of this SLSNe is a young magnetar.

I. INTRODUCTION

Superluminous supernovae (SLSNe) are a new type of supernovae and their luminosities are $\sim 10-100$ times larger than usual core-collapse supernovae (SNe) [1–3]. They are so bright that can be detected at redshifts of ≥ 3.5 [4]. The energy sources of these energetic explosions are still in debate and the widely discussed scenarios include ^{56}Ni decay, the interaction between ejecta and dense circumstellar media [5], and the spin-down of the nascent magnetar [6–8]. Theoretically, fast particle acceleration might occur soon after the supernova explosion, supposing the presence of interaction between the ejecta and pre-existing dense material [9] or there was a young, powerful pulsar wind nebula [10]. Therefore, SLSNe can be a new kind of GeV-TeV radiation source. Dedicated efforts have been made to search for γ -ray emission from SLSNe with the *Fermi* Large Area Telescope (*Fermi*-LAT) [11] observation data, including both individual analysis and stacking procedures, but no reliable signal has been detected so far [12, 13]. A variable γ -ray source, with an isotropic energy of $\sim 10^{51}$ erg ($D_L/156$ Mpc)² and a duration of ~ 2 years, was detected in the direction of a peculiar supernova iPTF14hls [14], where D_L is the luminosity distance of the source. If this γ -ray signal was from iPTF14hls, the GeV emission efficiency should be very high. Moreover, a quasi-stellar object SDSS J092054.04+504251.5, which is likely a blazar according to the infrared data, is found in the error circle of this GeV source. Therefore, it is unclear whether iPTF14hls is indeed a γ -ray emitter. Below we focus on the SLSNe SN 2017egm for two good reasons. One is that this event is one of the closest hydrogen-poor (Type-I) SLSNe at a redshift of $z = 0.0307$ ($D_L = 135$ Mpc) [15].

The other is that the γ -ray emission with a peak luminosity of $\sim 10^{43}$ erg s⁻¹ appearing at $t \sim 3$ months after the stellar explosion has been predicted in the modeling of its optical emission within the pulsar wind nebula scenario [16], which should have been detected by *Fermi*-LAT if it is indeed the case.

SN 2017egm was discovered by the *Gaia* satellite on 2017 May 23 [17]. The radio observation of SN 2017egm was carried out after the explosion, some constraints were obtained [18]. The *Swift* satellite [19] also observed the field of SN 2017egm with its X-ray telescope and the corresponding luminosity is $\sim 10^{41}$ erg s⁻¹ in the 0.3 – 10.0 keV band. The later analysis however found out that the X-ray emission was likely related to the starburst region in the center of NGC 3191 and hence irrelevant to SN 2017egm [18]. The γ -ray emission from SN 2017egm has also been searched and some constraints have been set in a wide energy range [13]. In this work, we carry out a dedicated analysis of the 15 years of *Fermi*-LAT data, and report a promising γ -ray counterpart of SN 2017egm along with some discussions and conclusions.

II. DATA ANALYSIS

We take the 15-year (2008 August 4 to 2023 August 4) *Fermi*-LAT Pass 8 data and the *Fermitools* to perform the analysis. The `evtype=3`, `evclass=128` events and the instrument response functions (IRFs) of `P8R3_SOURCE_V3` are employed. Owing to the poor angular resolution at low energies, only photons within the energy range of 500 MeV to 500 GeV are selected. The maximum zenith angle (Z_{max}) of events is 100° to reduce the contamination from the Earth Limb. In addition, the quality-filter cuts (`DATA_QUAL==1 && LAT_CONFIG==1`) are applied to ensure the data used are within good time intervals. The standard binned likelihood analysis method (implemented with the `gtlike` tool) is adopted in our approach.

* Corresponding author: yzfan@pmo.ac.cn

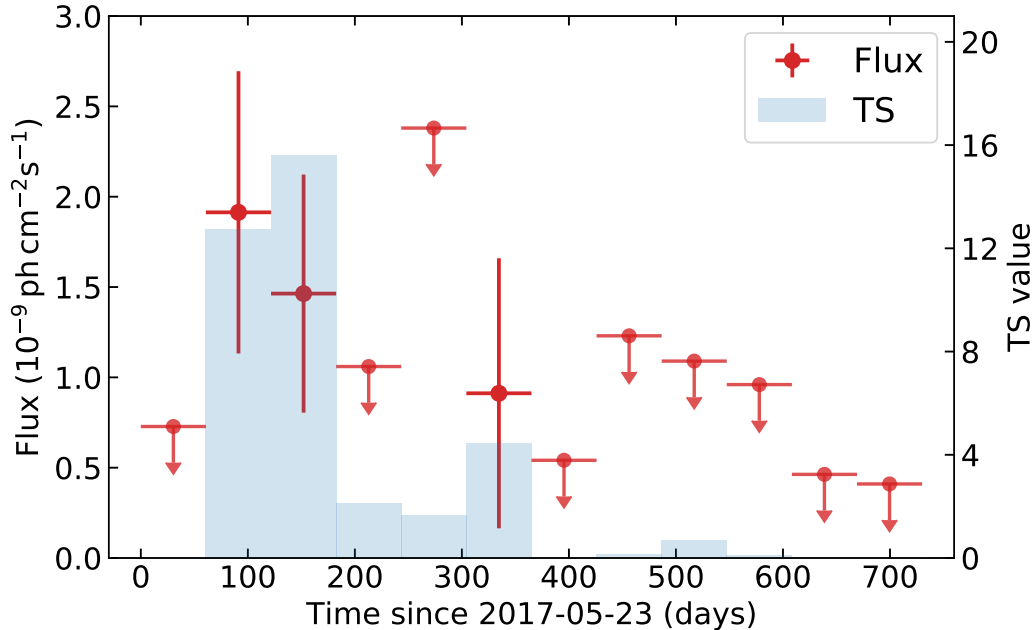


FIG. 1. Light curve of the γ -ray emission from the direction of SN 2017egm between 500 MeV and 500 GeV in 2-month bins. The zero point is 2017 May 23, the onset of the supernova. Shaded regions show the TS values (right axis). For TS values less than 4, 95% confidence level upper limits of fluxes are presented.

The region-of-interest (ROI) is taken to be a $14^\circ \times 14^\circ$ box centered at the target.

The script `make4FGLxml.py`¹ is applied to generate the initial background model, in which all 4FGL-DR4 [20] sources within 15° around the target and the two diffuse backgrounds (`gll_iem_v07.fits` and `iso_P8R3_SOURCE_V3_v1.txt`) are included. Due to the absence of SN 2017egm in current γ -ray catalogs, we add a new source at the optical position of SN 2017egm into the model file with a power-law spectrum (i.e. $dN/dE \propto E^{-\Gamma}$, where Γ is the spectral photon index) to model the supernova component. In the data analysis, the parameters of the 4FGL-DR4 sources within a 7° radius centered at the target as well as the normalization parameters of the two diffuse components are left free, while others are fixed to their 4FGL-DR4 values. The test statistic (TS = $2\Delta\log\mathcal{L}$) [21] is adopted to quantify the significance of a γ -ray source, where \mathcal{L} represents the maximum likelihood values and $\Delta\log\mathcal{L}$ is the log-likelihood difference between models with and without the new source.

III. RESULTS

Firstly, we fit the entire 15-year data and generate a residual TS map. Any excess in the TS map with a peak

TS value > 25 is treated as a new point source, and will be added into the background model with a power-law spectrum. Their positions are determined by the `gtfind-src` tool. After adding the sources into the background model, the data analysis is carried out once more. No significant γ -ray excess (TS ~ 0.7 with $\Gamma = 2.0$) is found in the direction of SN 2017egm. However, theoretical investigations predicted that the γ -ray emission just lasted weeks to months, depending on the SNe and the central compact object characteristics [10]. Then, we perform a fit of the two years data (from 2017 May 23 to 2019 May 23) after the explosion. The TS value is ~ 15.8 . Furthermore, the 2-month time bin light curve is derived. The 95% confidential level (C.L.) upper limit is calculated by `pyLikelihood UpperLimits` tool for the bin with TS < 4 . As shown in Fig 1, the TS values are small (< 4) in most time bins. However, for the second and third bins the TS values are larger than 12, in the time range from 2017 July 23 to 2017 November 23. The following analysis is conducted for this time interval. A localization analysis is performed for the new γ -ray source and the optimized coordinates are R.A. 154.79° and DEC. 46.40° with a 95% C.L. error radius of 0.18° . The SN 2017egm is only 0.06° away from the γ -ray source. Using the new γ -ray position, a strong γ -ray signal appears at the direction of SN 2017egm (see the (a) panel of Fig. 2). The TS value is ~ 30.1 and the corresponding γ -ray flux is $(1.9 \pm 0.6) \times 10^{-9}$ ph cm $^{-2}$ s $^{-1}$ between 500 MeV and 500GeV. If the γ -ray source is indeed related to SN 2017egm, the averaged isotropic γ -ray luminosity

¹ <https://fermi.gsfc.nasa.gov/ssc/data/analysis/user/make4FGLxml.py>

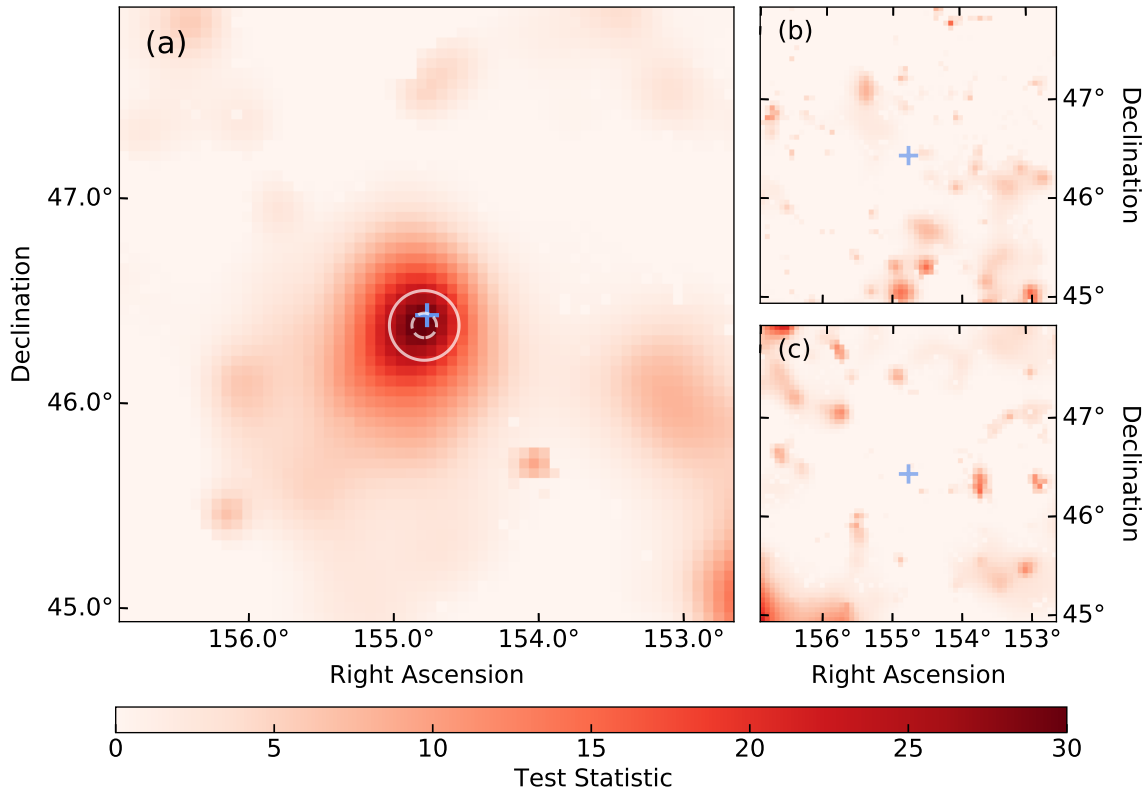


FIG. 2. TS maps for different epochs: (a) from 2017 July 23 to 2017 November 23, (b) before 2017 July 23, and (c) after 2017 November 23. The TS maps display $3^\circ \times 3^\circ$ region centered at SN 2017egm for the *Fermi*-LAT data between 500 MeV and 500 GeV. The optical position of SN 2017egm is represented by the blue cross symbol. The circles in panel (a) are the 68% (inner) and 95% (outer) error uncertainties of the γ -ray source localization.

in the period is $(9.0 \pm 2.4) \times 10^{42} (D_L/135 \text{ Mpc})^2 \text{ erg s}^{-1}$. The spectral energy distribution of the γ -ray source is presented in the Fig. 4 of the Supplementary Materials.

Furthermore, the data is divided into three parts (before 2017 July 23, from 2017 July 23 to 2017 November 23 and after 2017 November 23) to perform the likelihood analysis. For the first and the third parts, no significant γ -ray signal appears at the position of SN 2017egm (see the (b) and (c) panels of Fig. 2). However, a bright γ -ray signal (TS ~ 30.0) appears in the direction of SN 2017egm in the second period (see the (a) panel of Fig. 2), confirming that found in the 2-month bin γ -ray light curve.

IV. DISCUSSION AND CONCLUSION

The magnetar nebulae model of the SN 2017egm has been systematically discussed, and the self-consistent modeling predicted that the high-energy γ -ray emission would have a peak luminosity of $\sim 10^{43} \text{ erg s}^{-1}$ and hence may be detectable within a few months after the stellar explosion [13, 16]. In Fig. 3, we take the predicted

GeV emission light curve for a nebular magnetization $\varepsilon_B = 10^{-4}$ in the Figure 7 of Ref [16] to compare with the current data. Clearly, both the rise time, the peak luminosity as well as the decline behavior of the GeV emission are consistent with the prediction of the magnetar nebulae model. Such a consistence is in support of the millisecond magnetar central engine model of SN 2017egm.

Meanwhile, we have also searched for other possible counterparts according to the catalogs from the NASA/IPAC Extragalactic Database (NED) and SIMBAD Database. No prominent γ -ray emitters are found within the 95% error radius of the newly-identified γ -ray emission (see the Supplementary Material for the details). Such a null result is in support of the association of the γ -ray source with SN 2017egm.

We then suggest that SN 2017egm is a γ -ray emitter and the magnetars are the central engine of some superluminous supernovae, as initially suggested in [6–8]. Nevertheless, due to the strong self-absorption of the GeV-TeV emission accompanying the superluminous supernovae, the detection of such signal is challenging for *Fermi*-LAT. The situation will be changed in the future.

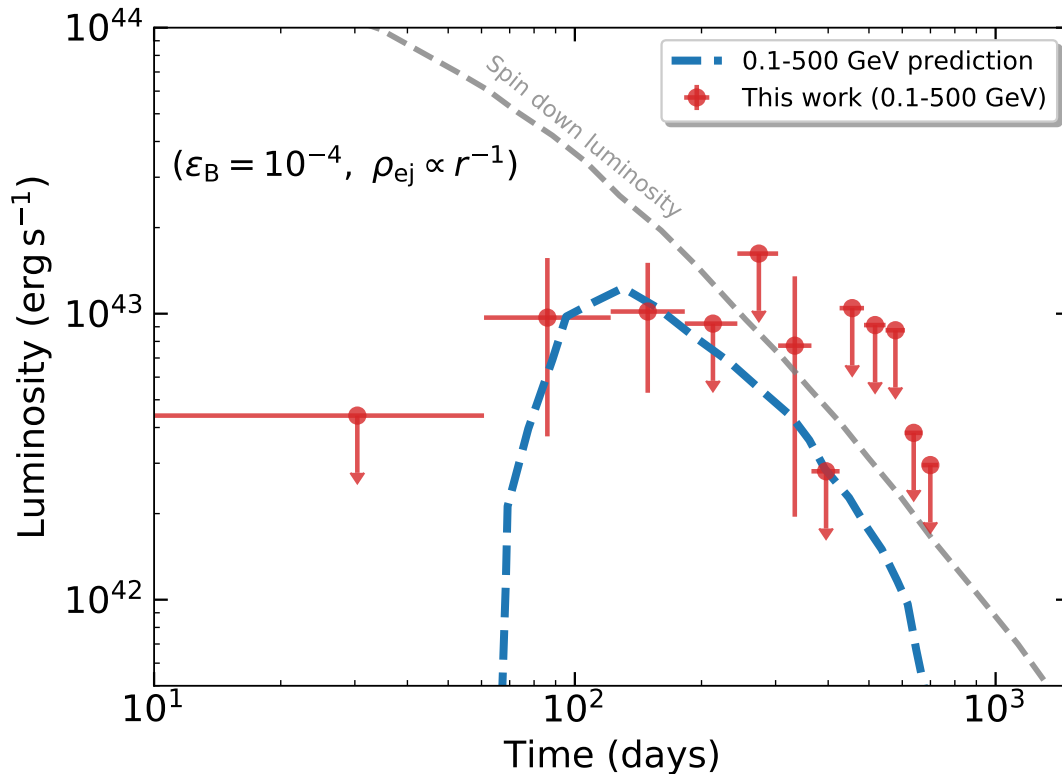


FIG. 3. The γ -ray light curve of magnetar-powered supernovae calculated for the nebula magnetization with $\varepsilon_B = 10^{-4}$ [16]. The 2-month bin light curve of SN 2017egm spanning 2 years after the explosion for 100 MeV to 500 GeV with a PLSuperExpCutoff spectral shape. The red points represent the integral energy flux and the red bars are upper limits.

The Very Large Area γ -ray Space Telescope (VLASt), one next generation γ -ray detector proposed recently, has an acceptance about 5 times larger than *Fermi*-LAT in the GeV-TeV energy range [22]. With such a sensitive detector, the GeV emission fainter than SN 2017egm will be recorded and a larger sample will be helpful in pinning down the fraction of the magnetars formed among the superluminous supernovae.

ACKNOWLEDGMENTS

This work is supported in part by the National Key Research and Development Program of China (No.

2022YFF0503302), the National Natural Science Foundation of China (No. 12103001 and No. 11921003), the New Cornerstone Science Foundation through the XPLOER PRIZE, and Anhui project (Z010118169).

-
- [1] R. M. Quimby *et al.*, “Hydrogen-poor superluminous stellar explosions,” *Nature* **474**, 487 (2011), arXiv:0910.0059.
 - [2] A. Gal-Yam, “Luminous Supernovae,” *Science* **337**, 927 (2012), arXiv:1208.3217.
 - [3] A. Gal-Yam, “The Most Luminous Supernovae,” *Ann. Rev. Astron. Astrophys.* **57**, 305 (2019), arXiv:1812.01428.
 - [4] J. Cooke, M. Sullivan, A. Gal-Yam, E. J. Barton, R. G. Carlberg, E. V. Ryan-Weber, C. Horst, Y. Omori, and C. G. Díaz, “Superluminous supernovae at redshifts of 2.05 and 3.90,” *Nature* **491**, 228 (2012), arXiv:1211.2003.
 - [5] T. J. Moriya, E. I. Sorokina, and R. A. Chevalier, “Superluminous supernovae,” *Space Sci. Rev.* **214**, 59 (2018), arXiv:1803.01875.

- [6] K. Maeda, M. Tanaka, K. Nomoto, N. Tominaga, K. Kawabata, P. A. Mazzali, H. Umeda, T. Suzuki, and T. Hattori, “The Unique Type Ib Supernova 2005bf at Nebular Phases: A Possible Birth Event of a Strongly Magnetized Neutron Star,” *Astrophys. J.* **666**, 1069 (2007), arXiv:0705.2713.
- [7] D. Kasen and L. Bildsten, “Supernova Light Curves Powered by Young Magnetars,” *Astrophys. J.* **717**, 245 (2010), arXiv:0911.0680.
- [8] S. E. Woosley, “Bright Supernovae from Magnetar Birth,” *Astrophys. J.* **719**, L204 (2010), arXiv:0911.0698.
- [9] K. Murase, T. A. Thompson, B. C. Lacki, and J. F. Beacom, “New class of high-energy transients from crashes of supernova ejecta with massive circumstellar material shells,” *Phys. Rev. D* **84**, 043003 (2011), arXiv:1012.2834.
- [10] K. Murase, K. Kashiyama, K. Kiuchi, and I. Bartos, “Gammay-Ray and Hard X-Ray Emission from Pulsar-aided Supernovae as a Probe of Particle Acceleration in Embryonic Pulsar Wind Nebulae,” *Astrophys. J.* **805**, 82 (2015), arXiv:1411.0619.
- [11] W. B. Atwood *et al.*, “The Large Area Telescope on the Fermi Gamma-Ray Space Telescope Mission,” *Astrophys. J.* **697**, 1071 (2009), arXiv:0902.1089.
- [12] N. Renault-Tinacci, K. Kotera, A. Neronov, and S. Ando, “Search for γ -ray emission from superluminous supernovae with the Fermi-LAT,” *Astron. Astrophys* **611**, A45 (2018), arXiv:1708.08971.
- [13] A. Acharyya *et al.*, “VERITAS and Fermi-LAT Constraints on the Gamma-Ray Emission from Superluminous Supernovae SN2015bn and SN2017egm,” *Astrophys. J.* **945**, 30 (2023), arXiv:2302.06686.
- [14] Q. Yuan, N.-H. Liao, Y.-L. Xin, Y. Li, Y.-Z. Fan, B. Zhang, H.-B. Hu, and X.-J. Bi, “Fermi Large Area Telescope detection of gamma-ray emission from the direction of supernova iPTF14hls,” *Astrophys. J. Lett.* **854**, L18 (2018), arXiv:1712.01043.
- [15] M. Nicholl, E. Berger, R. Margutti, P. K. Blanchard, J. Guillochon, J. Leja, and R. Chornock, “The Superluminous Supernova SN 2017egm in the Nearby Galaxy NGC 3191: A Metal-rich Environment Can Support a Typical SLSN Evolution,” *Astrophys. J.* **845**, L8 (2017), arXiv:1706.08517.
- [16] I. Vurm and B. D. Metzger, “Gamma-Ray Thermalization and Leakage from Millisecond Magnetar Nebulae: Toward a Self-consistent Model for Superluminous Supernovae,” *Astrophys. J.* **917**, 77 (2021), arXiv:2101.05299.
- [17] A. Delgado, D. Harrison, S. Hodgkin, M. V. Leeuwen, G. Rixon, and A. Yoldas, “GaiaAlerts Transient Discovery Report for 2017-05-25,” *Transient Name Server Discovery Report* **2017-591**, 1 (2017).
- [18] S. Bose *et al.*, “Gaia17biu/SN 2017egm in NGC 3191: The Closest Hydrogen-poor Superluminous Supernova to Date Is in a “Normal,” Massive, Metal-rich Spiral Galaxy,” *Astrophys. J.* **853**, 57 (2018), arXiv:1708.00864.
- [19] D. N. Burrows *et al.* (SWIFT Collaboration), “The Swift X-ray Telescope,” *Space Sci. Rev.* **120**, 165 (2005), arXiv:astro-ph/0508071.
- [20] J. Ballet, P. Bruel, T. H. Burnett, B. Lott, and The Fermi-LAT collaboration, “Fermi Large Area Telescope Fourth Source Catalog Data Release 4 (4FGL-DR4),” arXiv e-prints, arXiv:2307.12546 (2023), arXiv:2307.12546.
- [21] J. R. Mattox *et al.*, “The Likelihood Analysis of EGRET Data,” *Astrophys. J.* **461**, 396 (1996).
- [22] Y. Z. Fan *et al.*, “Very Large Area Gamma-ray Space Telescope (VLAST),” *Acta Astronomica Sinica* **63**, 27 (2022).
- [23] Gaia Collaboration *et al.*, “Gaia Data Release 3. Summary of the content and survey properties,” *Astron. Astrophys* **674**, A1 (2023), arXiv:2208.00211.
- [24] F. de Gasperin, H. T. Intema, and D. A. Frail, “A radio spectral index map and catalogue at 147-1400 MHz covering 80 per cent of the sky,” *Mon. Not. R. Astron. Soc.* **474**, 5008 (2018), arXiv:1711.11367.
- [25] S. Bruzewski, F. K. Schinzel, G. B. Taylor, and L. Petrov, “Radio Counterpart Candidates to Unassociated 4FGL-DR2 Sources,” *Astrophys. J.* **914**, 42 (2021), arXiv:2102.07397.
- [26] E. O. Ofek and D. A. Frail, “The Structure Function of Variable 1.4 GHz Radio Sources Based on NVSS and FIRST Observations,” *Astrophys. J.* **737**, 45 (2011), arXiv:1105.3479.
- [27] D. J. Helfand, R. L. White, and R. H. Becker, “The Last of FIRST: The Final Catalog and Source Identifications,” *Astrophys. J.* **801**, 26 (2015), arXiv:1501.01555.
- [28] B. Vollmer, B. Gassmann, S. Derrière, T. Boch, M. Louys, F. Bonnarel, P. Dubois, F. Genova, and F. Ochsenbein, “The SPECFIND V2.0 catalogue of radio cross-identifications and spectra. SPECFIND meets the Virtual Observatory,” *Astron. Astrophys* **511**, A53 (2010), arXiv:0912.4174.
- [29] H. T. Intema, P. Jagannathan, K. P. Mooley, and D. A. Frail, “The GMRT 150 MHz all-sky radio survey. First alternative data release TGSS ADR1,” *Astron. Astrophys* **598**, A78 (2017), arXiv:1603.04368.
- [30] R. G. McMahon, R. L. White, D. J. Helfand, and R. H. Becker, “Optical Counterparts for 70,000 Radio Sources: APM Identifications for the FIRST Radio Survey,” *Astrophys. J. Suppl.* **143**, 1 (2002), arXiv:astro-ph/0110437.
- [31] Y. A. Gordon *et al.*, “A Quick Look at the 3 GHz Radio Sky. II. Hunting for DRAGNs in the VLA Sky Survey,” *Astrophys. J. Suppl.* **267**, 37 (2023), arXiv:2303.12830.
- [32] Y. A. Gordon *et al.*, “A Quick Look at the 3 GHz Radio Sky. I. Source Statistics from the Very Large Array Sky Survey,” *Astrophys. J. Suppl.* **255**, 30 (2021), arXiv:2102.11753.
- [33] Y. Stein, B. Vollmer, T. Boch, G. Landais, P. Vannier, M. Brouty, M. G. Allen, S. Derriere, and P. Ocvirk, “The SPECFIND V3.0 catalog of radio continuum cross-identifications and spectra: Reaching lower frequencies,” *Astron. Astrophys* **655**, A17 (2021).
- [34] J. J. Condon, W. D. Cotton, E. W. Greisen, Q. F. Yin, R. A. Perley, G. B. Taylor, and J. J. Broderick, “The NRAO VLA Sky Survey,” *Astron. J.* **115**, 1693 (1998).
- [35] Y. Liu, D. R. Jiang, and M. F. Gu, “The Jet Power, Radio Loudness, and Black Hole Mass in Radio-loud Active Galactic Nuclei,” *Astrophys. J.* **637**, 669 (2006), arXiv:astro-ph/0510241.

SUPPLEMENTAL MATERIAL

Appendix A: Spectral analysis

We show in Fig. 4 the spectral energy distribution of the new γ -ray source for the data from 2017 July 23 to 2017 November 23. The energy range from 500 MeV to 500 GeV is divided into seven equal logarithmic energy bins. The blue shaded regions represent the TS values (right axis). For the energy bin with TS < 4, the 95% C.L. upper limit is presented. The power-law fit to the spectrum yields a spectral index of 2.6 ± 0.4 .

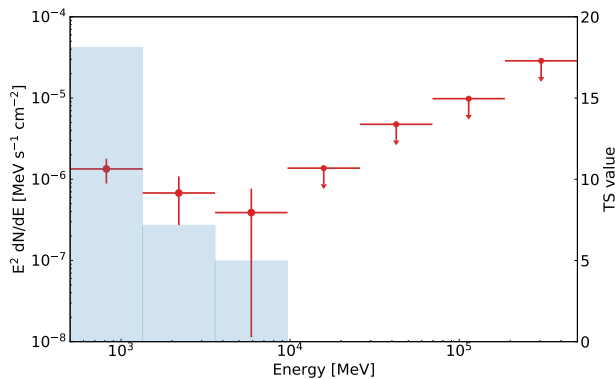


FIG. 4. Spectral energy distribution of the new γ -ray source.

Appendix B: The robustness of signal in *Fermi*-LAT data analysis

In order to understand the behavior of the γ -ray emission in the direction of SN 2017egm. A 1-year bin γ -ray light curve is extracted. From the Fig. 5, we can find that the TS value of the 10th bin (from 2017 August 4 to 2018 August 4) is ~ 23.8 and the TS values of the other bins are very small (< 4), which is consistent with the Fig. 2.

Further analysis indicated that the γ -ray emission is mainly concentrated in a period of 3-month, in the time range from 2017 July 23 to 2017 October 23. To further test the reliability of the γ -ray signal. We consider two different data selection situations, which include 1) the energy range from 300 MeV to 500 GeV, and 2) the $Z_{\max} = 90^\circ$. The results of the binned likelihood analysis are summarized in Table I.

In addition, we also perform an unbinned likelihood analysis to test the γ -ray signal. The photons are selected from 500 MeV to 500 GeV within a 7° region of interest (ROI) centered at the SN 2017egm. The data cuts are similar to the binned analysis, including zenith angles less than 100° and (DATA_QUAL == 1) && (LAT_CONFIG == 1). The results are also showed in Table I. For the four situations in Table I, the smallest TS value is 28.6

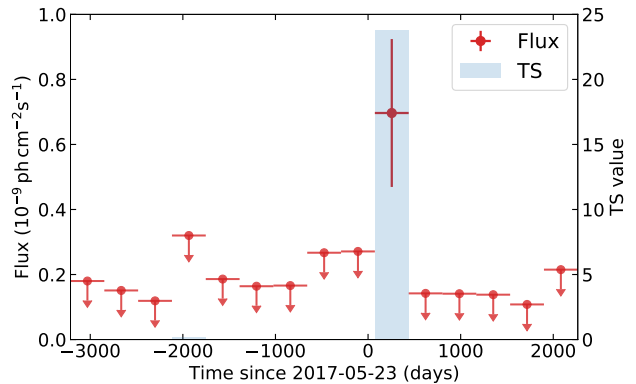


FIG. 5. Same as Fig. 1, but for one-year bin of the γ -ray light curve for 15-year *Fermi*-LAT data.

and the SN 2017egm are all within the 95% C.L. error radius.

To compare our results with that in Ref [13], we also perform a binned likelihood analysis with event selection similar to the Ref [13]. We select photons with energies from 100 MeV to 500 GeV and consider the same period from 2017 May 23 to 2020 August 21. To reduce the contamination from the Earth limb, only the events with zenith angle less than 90° are selected. The data are split into 200×200 spatial bins with 0.1° per pixel. A power-law spectrum ($dN/dE \propto E^{-\Gamma}$) with $\Gamma = 2.0$ is applied to fit the SN 2017egm. The model includes all 4FGL-DR4 sources within 20° around the target, together with the diffuse emission templates (gll_iem_v07.fits and iso_P8R3_SOURCE_V3_v1.txt).

First, we perform a fit of the entire data from 2017 May 23 to 2020 August 21. The TS value is ~ 4.6 and the energy flux upper limit is $1.1 \times 10^{-6} \text{ MeV cm}^{-2} \text{ s}^{-1}$ for the energy range from 100 MeV to 500 GeV. Then we split the data into seven time bins, the first bin is the first 90 days after the explosion and the other date is split into six bins (~ 6 -month of each bin). For the first bin, the energy flux upper limit is $3.6 \times 10^{-6} \text{ MeV cm}^{-2} \text{ s}^{-1}$ with a TS ~ 0.4 . The TS value of the first 6-month bin is ~ 9.5 , the corresponding energy flux upper limit is $4.6 \times 10^{-6} \text{ MeV cm}^{-2} \text{ s}^{-1}$. The peak TS value of the other 6-month bins is ~ 2.0 . These results are coincident with the Ref [13].

Appendix C: The lack of simultaneous activities of nearby sources

We searched for possible variable or burst activities from the nearby radio sources in the region of the γ -ray source. There is no strong evidence of simultaneous activities from nearby radio sources in the surveys conducted by the *GAIA*, *ZTF*, and *Chandra* satellites.

In our search for other potential contributions from burst or flare events in the vicinity of the γ -ray source

TABLE I. The likelihood analysis results for SN 2017egm (3-month period).

	Flux ($\times 10^{-9}$ ph cm $^{-2}$ s $^{-1}$)	TS	(RA,DEC) ^a ($^{\circ}$, $^{\circ}$)	R _d ^b ($^{\circ}$)	R _{95%} ^c ($^{\circ}$)
Binned, $Z_{\max} = 100^{\circ}$, [0.5 - 500 GeV]	2.8 ± 0.8	38.4	(154.80, 46.39)	0.07	0.18
Binned, $Z_{\max} = 90^{\circ}$, [0.5 - 500 GeV]	2.8 ± 0.8	31.7	(154.90, 46.33)	0.15	0.20
Binned, $Z_{\max} = 100^{\circ}$, [0.3 - 500 GeV]	3.1 ± 1.0	28.6	(154.79, 46.40)	0.06	0.14
Unbinned, $Z_{\max} = 100^{\circ}$, [0.5 - 500 GeV]	2.5 ± 0.6	32.5	(154.80, 46.38)	0.07	0.17

^a The γ -ray positions are determined by the *gtfindsrc* tool

^b R_d is the angular separation between the γ -ray position and the optical position of SN 2017egm

^c R_{95%} is the 95% error radius derived from the analysis.

using the GAIA survey, we found no significant luminous optical burst or flare in the *GAIA Data Release 3* catalogue [23], except for SN 2017egm. The *GAIA Data Release 3* covers the survey period from 2017-01-01 to 2018-10-15. While there are two quasar candidates with magnitudes of ~ 20 mag in the GAIA/G band photometry in the region, the amplitudes of their photometric light curves do not exceed ~ 1 mag. Therefore, the likelihood of these two quasar candidates (GAIA IDs: 810264031570565632, 810263378735530880) causing a burst event is very low.

We cross-matched the sources from the radio survey catalogs [24–34] with the ZTF Data Release 20² in a circular region with a radius of 0.2° located at R.A. 154.79° and DEC. 46.40° . Simultaneously, we searched and cross-matched the radio sources in the same region with the five Chandra X-ray exposures (Obsid: 19034, 19035, 19036, 19033, PI: Margutti; Obsid: 22501, PI: Lehmer). We combined the five Chandra observations using the script *merge_obs*³ from the Chandra standard software CIAO. Three X-ray sources were detected to have a significance $> 5\sigma$ with the CIAO script *wavdetect*⁴ in the merged observation and were cross-matched with radio sources within a radius of $9.0''$. Two of the three X-ray sources were cross-matched with the ZTF optical catalogue. The features of the three X-ray sources are listed in Table II.

We also considered the presence of strong jets in the cross-matched sources when assuming them to be quasars. We calculated the radio loudness $R = \frac{f_{\nu, 1.4\text{GHz}}}{f_{\nu, \text{ZTF-g}}}$ using the flux density values in Table II. The effective wavelength of the ZTF-g band is 472.2nm . The radio loudness of these ZTF sources in the γ -ray region falls between 'radio-quiet' and 'radio-loud' quasars based on

their radio and ZTF-g band emissions. Their radio loudness range is $R \sim 14 - 26$, which is lower than that of 'radio-loud' quasars ($R \sim 100$, [35]). The low radio loudness indicates that these assumed quasar candidates are unlikely to have strong jets.

To verify if the X-ray sources are associated with burst events, we assessed the flux variability of each source using the CIAO script *srcflux*⁵. The three sources exhibit faint X-ray emission ($1 \times 10^{-15} \sim 3 \times 10^{-14}$ erg s $^{-1}$ cm $^{-2}$) in the Chandra X-ray observations. We did not observe any obvious burst events in the X-ray light curves of the three X-ray sources.

Appendix D: Random sky simulations

We also performed random sky simulations to estimate the detection significance of the γ -ray signal. Considering the SN 2017egm is located at high galactic latitude ($|b| > 50^{\circ}$) and the nearest point source in 4FGL-DR4 to SN 2017egm is $\sim 2^{\circ}$, the blank-sky locations are randomly generated at high Galactic latitude ($|b| > 30^{\circ}$) and stay away from any 4FGL-DR4 catalog sources (no point sources are within 1° and no spatially extended sources are within 5°). For each blank-sky position, the corresponding time interval are randomly generated within the time range from 2008 August 4 to 2023 August 4 for a 4-month period. In total 20000 data sets are filtered and the binned likelihood analysis is performed for each data set. The distribution of $\sqrt{\text{TS}}$ is shown in Fig. 6. Due to the maximal TS value of the 20000 simulations is less than 25, the detection significance of the γ -ray signal (TS ~ 30.1) is at least 4σ .

² ZTF data release: <https://www.ztf.caltech.edu/ztf-public-releases.html>

³ *merge_obs*: https://cxc.harvard.edu/ciao/threads/merge_all/

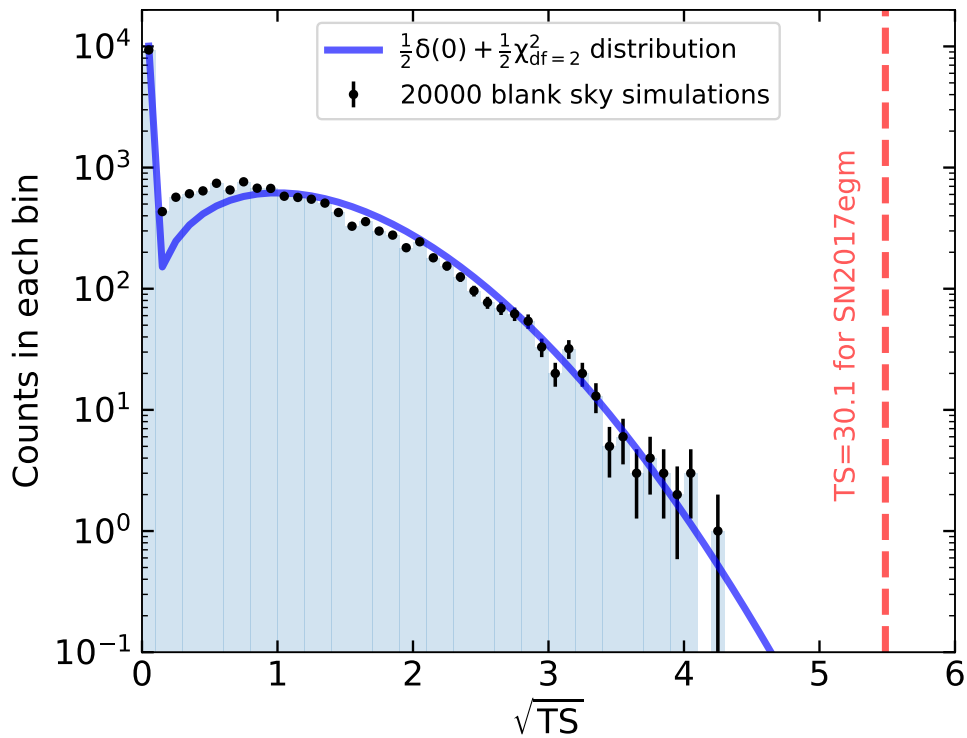
⁴ *wavdetect*: <https://cxc.cfa.harvard.edu/ciao/ahelp/>

wavdetect.html

⁵ *srcflux*: <https://cxc.cfa.harvard.edu/ciao/ahelp/srcflux.html>

TABLE II. The features of the three cross-matched Chandra X-ray sources in the direction of the GeV γ -ray transient.

cross-match	# of sources cross-matched	band	position (RA, DEC)	offset to radio obj (")	flux density (erg/s/cm ² /Hz)	burst event? (light curve)
Radio Source 1 (154.77099, 46.45466): NVSS, $f_{\nu,1.4\text{GHz}} = 1.0 \times 10^{-25}$ erg/s/cm ² /Hz, Ref[24]						
Chandra	1/1	0.5-7.0 keV	154.76867, 46.45439	8.4''	$2.9 \pm 4.9 \times 10^{-32}$	no
ZTF	1/1	g	154.77141, 46.45413	2.4''	$5.79^{+6.39}_{-1.47} \times 10^{-27}$	no
ZTF	1/1	r	154.77141, 46.45413	2.4''	$1.12^{+1.34}_{-0.28} \times 10^{-26}$	no
ZTF	1/1	i	154.77141, 46.45413	2.4''	$1.46^{+3.85}_{-2.95} \times 10^{-26}$	no
Radio Source 2 (154.74294, 46.45402): NVSS, $f_{\nu,1.4\text{GHz}} = 3.7 \times 10^{-26}$ erg/s/cm ² /Hz, Ref[26]						
Chandra	1/1	0.5-7.0 keV	154.74325, 46.45343	2.3''	$3.95 \pm 7.0 \times 10^{-32}$	no
ZTF	1/3	g	154.74283, 46.45441	1.4''	$2.60^{+1.08}_{-0.89} \times 10^{-27}$	no
ZTF	1/3	r	154.74283, 46.45441	1.4''	$4.38^{+1.68}_{-1.71} \times 10^{-27}$	no
ZTF	2/3	r	154.74167, 46.45414	4.6''	$8.02^{+7.77}_{-3.02} \times 10^{-27}$	no
ZTF	2/3	i	154.74167, 46.45414	4.6''	$1.02^{+0.37}_{-0.16} \times 10^{-26}$	no
ZTF	3/3	g	154.74360, 46.45497	4.2''	$1.41^{+1.12}_{-0.56} \times 10^{-27}$	no
Radio Source 3 (154.56401, 46.44057): FIRST, $f_{\nu,1.4\text{GHz}} = 1.3 \times 10^{-26}$ erg/s/cm ² /Hz, Ref[30]						
Chandra	1/1	0.5-7.0 keV	154.5642600, 46.4411149	2.2''	$7.36 \pm 12.4 \times 10^{-32}$	no
ZTF	0/0	-	-	-	-	-

FIG. 6. $\sqrt{\text{TS}}$ distribution of 20000 random sky simulations.